Effective conductivity of suspensions of overlapping spheres

In Chan Kim
Department of Mechanical and Aerospace Engineering, North Carolina State University, Raleigh, North Carolina 27695-7910

S. Torquato[a)]
Department of Mechanical and Aerospace Engineering and Department of Chemical Engineering, North Carolina State University, Raleigh, North Carolina 27695-7910

(Received 30 September 1991; accepted for publication 6 December 1991)

An accurate first-passage simulation technique formulated by the authors [J. Appl. Phys. **68**, 3892 (1990)] is employed to compute the effective conductivity σ_e of distributions of penetrable (or overlapping) spheres of conductivity σ_2 in a matrix of conductivity σ_1. Clustering of particles in this model results in a generally intricate topology for virtually the entire range of sphere volume fractions ϕ_2 (i.e., $0 \leqslant \phi_2 \leqslant 1$). Results for the effective conductivity σ_e are presented for several values of the conductivity ratio $\alpha = \sigma_2/\sigma_1$, including superconducting spheres ($\alpha = \infty$) and perfectly insulating spheres ($\alpha = 0$), and for a wide range of volume fractions. The data are shown to lie between rigorous three-point bounds on σ_e for the same model. Consistent with the general observations of Torquato [J. Appl. Phys. **58**, 3790 (1985)] regarding the utility of rigorous bounds, one of the bounds provides a good estimate of the effective conductivity, even in the extreme contrast cases ($\alpha \gg 1$ or $\alpha \simeq 0$), depending upon whether the system is below or above the percolation threshold.

I. INTRODUCTION

Determination of effective properties (e.g., transport, mechanical, and electromagnetic properties) of disordered composite materials is a subject of great importance in science and engineering, and in recent years has attracted considerable attention in the literature (see Refs. 1 and 2 and references therein). In order to predict the effective properties, an infinite set of correlation functions that statistically characterize the microstructure must be known.[2] In practice, such complete statistical information is never known, making exact determination of the effective property for arbitrary volume fractions and phase properties generally impossible, even for the simplest class of problems, i.e., steady-state diffusion properties such as conductivity, dielectric constant, and diffusion constant: the focus of this study. There are essentially two theoretical approaches in predicting the properties of arbitrary random composites: effective-medium approximations[3,4] and rigorous bounding techniques.[1,2,5–8] The accuracy of these theories can be ascertained by comparing them to "exact" data for well-defined model microstructures as obtained from computer-simulation experiments.

It is only very recently that such benchmark results have been obtained for continuum (off lattice) models of random composite media.[9–13] The authors in particular have devised a first-passage-time simulation technique to compute "exactly" the effective conductivity σ_e of general models of n-phase heterogeneous media having phase conductivities $\sigma_1, \sigma_2, \ldots, \sigma_n$, where σ_i can be finite or infinite.[10] The method was shown to yield effective conductivities for periodic arrays of particles that were in excellent agreement with known exact results for such idealized models, for a wide range of conditions (including superconducting particles), validating the accuracy of the simulation technique.[10–12] The procedure was also employed to compute the effective conductivities of random arrays of nonoverlapping, oriented cylinders[10] and of nonoverlapping spheres.[11]

In this paper, we seek to apply the first-passage-time method to determine the effective conductivity of identical fully penetrable spheres (i.e., spatially uncorrelated spheres). This model is sometimes referred to as "overlapping spheres," "randomly centered spheres," or as the "Swiss-cheese" model. For simplicity we will refer to it as overlapping spheres. Figure 1 shows a two-dimensional realization of overlapping particles. Overlapping-particle systems have a richer topology than the "equilibrium" nonoverlapping-particle systems examined by the authors in Refs. 10–12. For example, the latter model possesses only monomers (clusters of size one) for the entire range of particle volume fractions ϕ_2, except at the maximum volume fraction corresponding to the random close-packing value,[14] i.e., the percolation threshold $\phi_2^c \simeq 0.63$. By definition, an infinite cluster exists in any statistically homogeneous system at the percolation threshold. In contrast, clusters of various sizes (e.g., monomers, dimers, trimers, etc.) are present in systems of identical overlapping spheres at finite volume fractions below the percolation-threshold value[15] $\phi_2^c \simeq 0.3$. Nontrivial clustering occurs above the threshold as well, indeed, up to the maximum volume fraction of $\phi_2 = 1$. The system is, in fact, bicontinuous in the range $0.3 < \phi_2 < 0.97$: the value $\phi_2 = 0.97$ corresponding to the value at which the space exterior to the spheres fails to percolate.[16] The overlapping-sphere system is a prototypical model that has been employed extensively

[a)]Author to whom all correspondence should be addressed.

 0021-8979/92/062727-09$04.00

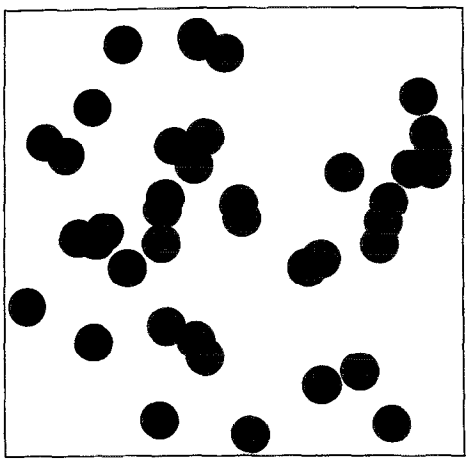

FIG. 1. A two-dimensional realization of overlapping particles. Here there are 12 monomers, three dimers, and six trimers.

in the study of the effective properties of heterogeneous systems[2,17,18] and of continuum-percolation theory.[15,19] It is therefore a model for which benchmark results for the effective conductivity are highly desirable.

In the ensuing section we briefly describe first-passage-time equations in the homogeneous regions and near-interface boundaries. We then discuss the simulation procedure for the model of overlapping spheres. In the following section we present our simulation data for the effective conductivity for values of the conductivity ratio $\alpha = \sigma_2/\sigma_1 = 0$, 10, 50, and ∞, for a wide range of sphere volume fractions. This data is compared to previously obtained rigorous three-point bounds on σ_e for the same model.

II. FIRST-PASSAGE-TIME FORMULATION

A general formulation to obtain exactly the effective conductivity σ_e for general isotropic n-phase composites having phase conductivities σ_1, σ_2,..., σ_n was originally given by the authors[10] in terms of certain averages of Brownian motion trajectories. The appropriate first-passage-time equations that apply in the homogeneous phases and at the multiphase interface for d-dimensional media of arbitrary microstructure was then derived and applied to compute the effective conductivities σ_e of equilibrium distributions of two-dimensional hard disks.[10] It was subsequently applied to compute σ_e of equilibrium distributions of three-dimensional hard spheres.[11] Since the formulation is general, it can be also applied for distributions of overlapping spheres which, as indicated in Sec. I, is topologically much more complex than nonoverlapping-sphere systems. Here we briefly present the appropriate formulation for the model of interest, that is, of the distribution of overlapping spheres of conductivity σ_2 in a matrix of conductivity σ_1.

A. Effective conductivity

For a Brownian particle (conduction tracer) moving in a homogeneous medium of conductivity σ, the mean hitting time $\tau(R)$, which is defined to be the mean time taken for a Brownian particle initially at the center of a sphere of radius R to hit the surface for the first time, is $\tau(R) = R^2/6\sigma$.[10] The conductivity σ of an infinite medium is therefore given by

$$\sigma = [R^2/6\tau(R)]|_{R\to\infty}. \tag{1}$$

Likewise, the effective conductivity σ_e of a composite medium can be expressed as

$$\sigma_e = [X^2/6\tau_e(X)]|_{X\to\infty}. \tag{2}$$

Here $\tau_e(X)$ is the total mean time associated with the total mean-square displacement X^2 of a Brownian particle moving in the composite medium.

In the actual computer simulation, in most cases where the Brownian particle is far from the two-phase interface, we employ the time-saving first-passage-time technique[10–12] which is now described. First, one constructs the largest imaginary concentric sphere of radius R around the diffusing particle which just touches the multiphase interface. The Brownian particle then jumps in one step to a random point on the surface of this imaginary concentric sphere and the process is repeated, each time keeping track of R_i^2 (which is equivalent to keeping track of the mean hitting time τ) where R_i is the radius of the ith first passage sphere, until the particle is within some prescribed very small distance of two-phase interface. At this juncture, we need to compute not only the mean hitting time $\tau_s(R)$ associated with imaginary concentric sphere of radius R in the small neighborhood of the interface but also the probability of crossing the interface. Both of these quantities are functions of σ_1, σ_2 and the local geometry. Thus the expression for the effective conductivity used in practice is given by[10,11]

$$\sigma_e = \left.\frac{\langle \Sigma_i R_i^2 + \Sigma_j R_j^2 + \Sigma_k R_k^2\rangle}{6\langle \Sigma_i \tau_1(R_i) + \Sigma_j \tau_2(R_j) + \Sigma_k \tau_s(R_k)\rangle}\right|_{X\to\infty}, \tag{3}$$

since $X^2 = \langle \Sigma_i R_i^2 + \Sigma_j R_j^2 + \Sigma_k R_k^2\rangle$. Here $\tau_1(R)$ $[\tau_2(R)]$ denotes the time for a Brownian particle to make a first passage in a homogeneous sphere of radius R of conductivity σ_1 (σ_2), the summations over the subscript i and j are for the Brownian paths in phase 1 and phase 2, repectively, and the summation over the subscript k is for the Brownian paths crossing the interface boundary.

Since $\tau_1(R) = R^2/6\sigma_1$ and $\tau_2(R) = R^2/6\sigma_2$, we have

$$\frac{\sigma_e}{\sigma_1} = \left.\frac{\langle \Sigma_i \tau_1(R_i) + \Sigma_j \tau_1(R_j) + \Sigma_k \tau_1(R_k)\rangle}{\langle \Sigma_i \tau_1(R_i) + \Sigma_j \tau_1(R_j)/\alpha + \Sigma_k \tau_s(R_k)\rangle}\right|_{X\to\infty}. \tag{4}$$

Here $\alpha = \sigma_2/\sigma_1$ is the conductivity ratio. Note that, for an infinite medium, the initial position of the Brownian particle is arbitrary. Equation (4) is the basic equation to be used to compute the effective conductivity σ_e of distributions of overlapping spheres.

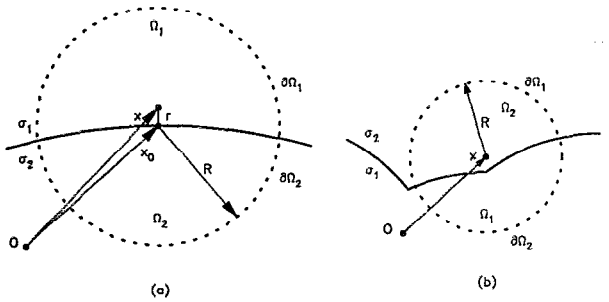

FIG. 2. Two-dimensional depiction of the small neighborhood of (a) smooth and (b) nonsmooth interface boundaries which are the surfaces between the matrix of conductivity σ_1 and overlapping spheres of conductivity σ_2.

B. Brownian particle crossing the interface

The first-passage quantities (described below) when the Brownian particle is very close to the generally irregular interface must be determined. We first discuss the first-passage quantities for the special case of a smoothly curved interface and subsequently for the case of a generally irregular interface.

Let $\Omega = \Omega_1 \cup \Omega_2$ be the small spherical first-passage region of radius R centered at the interface at position $\mathbf{x}_0$, where Ω_i is the portion of Ω that is in phase i, and $\partial\Omega_i$ is the surface of Ω_i excluding the two-phase interface [see Fig. 2(a)]. The key questions are: (i) What is the probability p_1 (p_2) that the Brownian particle initially at $\mathbf{x}$ near $\mathbf{x}_0$ eventually first arrives at the surface $\partial\Omega_1$ (the surface $\partial\Omega_2$), and (ii) what is the mean hitting time τ_s for the Brownian particle initially at $\mathbf{x}$ to hit $\partial\Omega$ ($= \partial\Omega_1 \cup \partial\Omega_2$) for the first time?

The first-passage-time quantities p_i and τ_s are solutions of certain Laplace and Poisson boundary-value problems, respectively, as obtained by the authors.[10–12] They specifically gave analytical expressions for p_1, p_2, and τ_s in case of a generally curved interface [Fig. 2(a)], which can be summarized as follows:

$$p_1 = \begin{cases} \dfrac{A_1}{A_1+\alpha A_2}\left(1+\alpha \displaystyle\sum_{m=0}^{\infty} B_{2m+1}\epsilon^{2m+1}\right), & \text{for } \mathbf{x}\subset\Omega_1, \\ \dfrac{A_1}{A_1+\alpha A_2}\left(1- \displaystyle\sum_{m=0}^{\infty} B_{2m+1}\epsilon^{2m+1}\right), & \text{for } \mathbf{x}\subset\Omega_2, \end{cases} \tag{5}$$

$$p_2 = 1-p_1,$$

$$= \begin{cases} \dfrac{\alpha A_2}{A_1+\alpha A_2}\left(1-\alpha \displaystyle\sum_{m=0}^{\infty} B_{2m+1}\epsilon^{2m+1}\right), & \text{for } \mathbf{x}\subset\Omega_1, \\ \dfrac{\alpha A_2}{A_1+\alpha A_2}\left(1+ \displaystyle\sum_{m=0}^{\infty} B_{2m+1}\epsilon^{2m+1}\right), & \text{for } \mathbf{x}\subset\Omega_2, \end{cases} \tag{6}$$

and

$$\tau_s = \begin{cases} \dfrac{R^2}{6\sigma_1}\dfrac{V_1+V_2}{V_1+\alpha V_2}\left(1-\dfrac{3\alpha-1}{2}\epsilon^2+\dfrac{\alpha-1}{2}\displaystyle\sum_{m=0}^{\infty} C_{2m+1}\epsilon^{2m+1}\right), & \text{for } \mathbf{x}\subset\Omega_1, \\ \dfrac{R^2}{6\sigma_1}\dfrac{V_1+V_2}{V_1+\alpha V_2}\left(1+\dfrac{\alpha-3}{2\alpha}\epsilon^2-\dfrac{\alpha-1}{2\alpha}\displaystyle\sum_{m=0}^{\infty} C_{2m+1}\epsilon^{2m+1}\right), & \text{for } \mathbf{x}\subset\Omega_2, \end{cases} \tag{7}$$

where

$$B_{2m+1} = \frac{(-1)^m(2m)!}{2^{2m+1}(m!)^2}\frac{4m+3}{m+1}$$

and

$$C_{2m+1} = \frac{(-1)^{m+1}(2m)!}{2^{2m+1}(m!)^2}\frac{3(4m+3)}{(2m-1)(m+2)(m+1)}.$$

Here $A_i (i = 1,2)$ is the area of the surface $\partial\Omega_i$ in phase i, V_i is the volume of region Ω_i, and $\epsilon = r/R = |\mathbf{x} - \mathbf{x}_0|/R$. Note that Eqs. (5)–(7) were originally developed for the generally smoothly curved interface [or interface of an arbitrarily shaped convex monomer as in Fig. 2(a)].

In the present model of suspensions of overlapping spheres, however, the interface generally consists of intersecting sphere surfaces. The Brownian particle, therefore, may at times be very near to the region of intersection between two or more spheres in such a way that the first-passage sphere encompasses intersecting sphere surfaces [see Fig. 2(b)]. Even though the accurate solutions (5)–(7) can be always used by making the first-passage sphere arbitrarily small, it is more practical from a simulation point of view to use modifications of these results when the first-passage sphere encompasses intersecting sphere surfaces. This is done by noticing the second terms in the square bracket of the right-hand side (rhs) of Eqs. (5) and (6) are of order $O(\epsilon)$ and that the second and third terms in the square bracket of the rhs of Eq. (7) are of order $O(\epsilon^2)$. The modifications to (5)–(7) in such situations as depicted in Fig. 2(b) are then as follows:

$$p_1 = \frac{A_1}{A_1+\alpha A_2}[1+O(\epsilon)] = \frac{A_1}{A_1+\alpha A_2}, \tag{8}$$

$$p_2 = 1 - p_1 = \frac{\alpha A_2}{A_1 + \alpha A_2}[1 + O(\epsilon)] = \frac{\alpha A_2}{A_1 + \alpha A_2}, \tag{9}$$

and

$$\tau_s = \frac{R^2}{6\sigma_1}\frac{V_1 + V_2}{V_1 + \alpha V_2}[1 + O(\epsilon^2)] = \frac{R^2}{6\sigma_1}\frac{V_1 + V_2}{V_1 + \alpha V_2}. \tag{10}$$

In employing Eqs. (8)–(10), the center of the first-passage sphere is at $\mathbf{x}$ instead of $\mathbf{x}_0$ at the interphase boundary. Equations (8)–(10) imply that the effects of irregularity of the local geometry of the interface boundary on p_1, p_2, and τ_s are accounted for only by the area ratio A_2/A_1 and by the volume ratio V_2/V_1, respectively and that they can be therefore used for generally irregular interface boundaries. Note that these equations were also employed in our studies of hard particles[10,11] when the particles were close to one another (i.e., high sphere concentrations) and were found to yield highly accurate results for the respective effective conductivities.

C. Brownian particle at the surface of superconducting phase

Consider suspensions of superconducting spheres ($\alpha = \infty$). If $\alpha = \infty$, Eqs. (5)–(10) yield trivial answers: $p_1 = 0, p_2 = 1$, and $\tau_s = 0$. This implies that the Brownian particle at the interface boundary always gets trapped in the superconducting phase and never escapes from there, spending no time in the process. This is undesirable from a simulation standpoint since we need to investigate the Brownian particle behavior in the large time limit. The essence of the first-passage time technique for this case, developed by Kim and Torquato,[10] is as follows: (i) A Brownian particle moves in the same fashion as the Brownian motion in the homogeneous region if it is in the nonsuperconducting region far from the interface boundary; (ii) once it is very close to the interface boundary (in practice, within a prescribed small distance from the interface boundary), it is absorbed into the superconducting cluster and jumps out of the cluster after spending time τ_s; (iii) if it happens to be inside the superconducting cluster, the procedure of (ii) is applied. Note that the computation of τ_s in step (ii) is crucial to the technique and is now described below.

In Fig. 3, a schematic diagram of a superconducting dimer (i.e., a cluster made of two spheres of radius a) is drawn. In order to use the first-passage algorithm in such instances, whenever the Brownian particle is within a small prescribed distance $\delta_1 a$ ($\delta_1 \ll 1$) from the interface, instead of computing V_1 and V_2 in Eq. (7) or Eq. (10), we need to compute the volumes V_I and V_O. The quantity V_I is the inner union volume of two spheres of radius $a(1 + \delta_I)$, where $\delta_I a$ is the actual distance of the Brownian particle from the interface boundary, while V_O is the outer union volume of two spheres of radius $a(1 + \delta_2)$, where δ_2 is another prescribed number such that $0 \leqslant \delta_I \leqslant \delta_1 < \delta_2 < 1$. The details on how to compute V_I and V_O are described in the following section. The expression for τ_s is then given by[10]

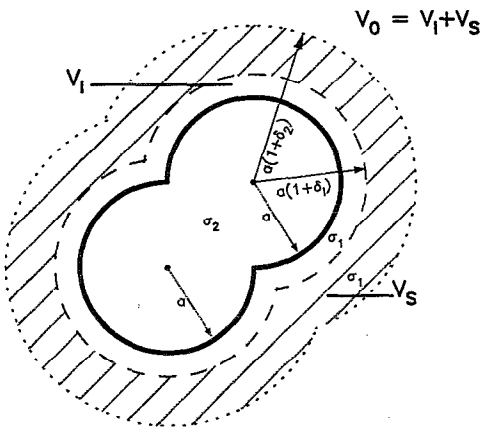

FIG. 3. An illustration of a cluster made of two overlapping particles for the case of $\alpha = \sigma_2/\sigma_1 = \infty$. Here V_I is the union volume of two overlapping particles of radius a plus the imaginary concentric inner shell of thickness $\delta_I a$ (of conductivity σ_1) and V_s is the volume of the imaginary concentric outer shell of thickness $\delta_2 a$ (of conductivity σ_1), respectively. V_O is the sum of V_I and V_s.

$$\tau_s = \tau_1[1 - (V_I^{2/3}/V_O^{2/3})], \tag{11}$$

where τ_1 is the mean hitting time for the Brownian particle initially at the center of mass of the homogeneous region of volume V_O and conductivity σ_1 to first strike the surface of this volume.

III. SIMULATION DETAILS

Here we apply the Brownian motion formulation to compute the effective conductivity σ_e of random distributions of overlapping spheres of conductivity σ_2 in a matrix of conductivity σ_1. We consider the cases of phase conductivity ratio $\alpha = \sigma_2/\sigma_1 = 0$, 10, 50, and ∞. Before presenting these simulation results, we first describe the simulation procedure in some detail.

Obtaining the effective conductivity σ_e from computer simulations is a two-step process: (i) First, one must generate realizations of the random heterogeneous medium; (ii) second, employing the Brownian motion algorithm, one determines the effective conductivity for each realization (using many Brownian particles) and then averages over a sufficiently large number of realizations to obtain σ_e.

A simple and efficient means of generating configurations of overlapping spheres at volume fraction ϕ_2, is to randomly and sequentially place each sphere of radius a in a cubical cell of size L^3 until the desired density $\rho = N/L^3$ is reached. For all the computer-generated configurations considered, the number of spheres in a configuration N was taken to be $N = 125$–500 in almost all cases. In order to study finite-size effects in the superconducting cases ($\alpha = \infty$), we sometimes examined systems with N up to 20 000 (see discussion below). Notice that for an

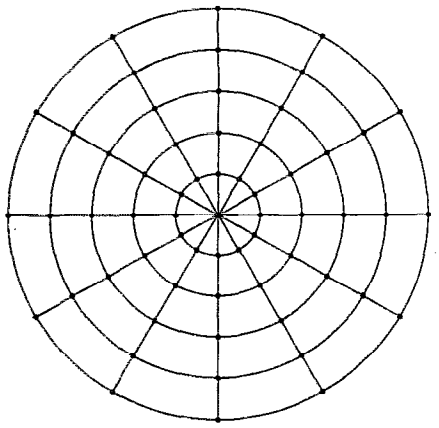

FIG. 4. Two-dimensional regularly arranged template used by Smith and Torquato (see Ref. 20) to measure two-point correlation function. A similar measuring template is used in this paper except that the measuring points are chosen randomly and uniformly.

equilibrium distribution of overlapping spheres, the volume fraction ϕ_2 is related to the density ρ by

$$\phi_2 = 1 - \exp(-\eta) = 1 - \exp[-(4\pi/3)\rho a^3], \quad (12)$$

where the reduced density η is defined by the relation $\eta = 4\pi\rho a^3/3$.

The essence of the Brownian motion algorithm has been described in Sec. II. Here we need to be more specific about the conditions under which the Brownian particle is considered to be in the small neighborhood of the interface and hence when the mean time τ_s and probabilities p_1 and p_2 need to be computed. An imaginary thin concentric shell of radius $a(1 + \delta_1)$ is drawn around each cluster consisted of overlapping spheres of radius a. We first describe the algorithm for the case of the distributions of clusters consisting of nonsuperconducting ($\alpha \neq \infty$) overlapping spheres. If a Brownian particle enters this thin shell, then we employ the first-passage-time equations (5)–(10), where the local phase surface area ratio A_2/A_1 and the local phase volume ratio V_2/V_1 of the imaginary sphere should be computed. However, for the case of nonsmooth interface boundary as shown in Fig. 2(b), the exact determination of A_2/A_1 and V_2/V_1 is generally impossible. In order to accomplish this, we introduce here what we call the template method. The idea was originally adopted by Smith and Torquato[20] where they placed an imaginary measuring template in the two-phase medium to determine whether two points separated by distance r belong to the same phase and then to compute numerically the two-point correlation function $S_2(r)$. They chose the measuring points at regular sites of the template (see Fig. 4). We instead choose the measuring points uniformly and randomly. First, in order to compute A_2/A_1, we uniformly and randomly throw M_A points on the surface of the imaginary first-passage sphere of radius $R = \delta_2 a$ and count the number of occasions $M_{A,1}$ ($M_{A,2}$) that these points fall on $\partial\Omega_1$ ($\partial\Omega_2$) [see Fig. 2(b)]. The area ratio A_2/A_1 is then determined to be $M_{A,2}/M_{A,1}$. Next, M_V points are thrown inside the first passage sphere and the number of occasions $M_{V,1}$ ($M_{V,2}$) that these points fall in Ω_1 (Ω_2) is counted. The volume ratio V_2/V_1 is then determined to be $M_{V,2}/M_{V,1}$. Of course, for the case of a smooth interface boundary as shown in Fig. 2(a), these quantities are exactly computed analytically without any difficulty.

In case of superconducting clusters ($\alpha = \infty$), in order to use Eq. (11), we need to compute the volumes V_I, V_O associated with each cluster (see Fig. 3). Since the spheres are free to overlap, the shape of the clusters can be arbitrarily irregular even though the constituents are spherical. An exact determination of the volumes associated with the generally irregular cluster is not easy especially if the cluster is made of four or more overlapping spheres. In order to overcome this difficulty, we devised what we call the pixel method, in which we tesselate the unit cell into a large number of cubical pixels and identify each pixel by the cluster (or matrix) to which it belongs. This is easily done with the aid of the so-called Hoshen–Kopelman algorithm.[21] The volume of a cluster is simply determined to be the number of pixel centers contained within the cluster. The concentric shell of thickness $\delta_I a$ surrounding each cluster is very small ($\delta_I \leqslant \delta_1 \ll 1$). Therefore, the volume of the inner cluster V_I is taken to be the number of pixel centers that belongs to the cluster made of spheres of radius a [instead of $a(1 + \delta_I)$]. This is done since it is difficult to compute V_I exactly because δ_I varies continuously between 0 and δ_1. In practice, choosing a instead of the exact $a(1 + \delta_I)$ in computing V_I involves little error and, in fact, its effect on the effective conductivity σ_e was found to be well within statistical fluctuations. In contrast, the volume of the outer cluster V_O (see Fig. 3) is computed directly by growing the radius of each constituent sphere from a to $a(1 + \delta_2)$ and counting the number of pixel centers belonging to the resultant bigger cluster. Once all the outer cluster volumes are computed, then the Brownian particles are released. Whenever a Brownian particle comes close to a superconducting cluster, Eq. (11) is used with the appropriate V_I and V_O.

After a sufficiently large total mean-square displacement, Eq. (4) is then employed to yield the effective conductivity for each Brownian trajectory and each realization. Many different Brownian trajectories are considered per realization. The effective conductivity σ_e is finally determined by averaging the conductivities over all realizations. Finally, note that the so-called grid method[22] was used to reduce the computation time needed to check if the walker is near a cluster. It enables one to check for spheres in the immediate neighborhood of the walker instead of checking each sphere.

In our simulations, we have taken $\delta_1 = 0.0001$ and $\delta_2 = 0.01$. We considered 100–250 equilibrium realizations and 100 Brownian particles per realization, and have let the dimensionless total mean-square displacement X^2/a^2 vary from 1 to 10, depending on the value of ϕ_2 and α.

In the superconducting instance ($\alpha = \infty$), we studied finite-size effects, even though we only considered the range $0 \leqslant \phi_2 \leqslant 0.28$, where the threshold $\phi_2^c \simeq 0.3$. For the range $\phi_2 < 0.25$, the number of particles $N = 500$ turned

out to be sufficiently large, i.e., σ_e did not change (within statistical errors) for $N > 500$. We, therefore, computed σ_e for systems with $N = 500$ for this range of volume fractions. However, for the range $\phi_2 \geqslant 0.25$, finite-size effects were observed even in very large systems with $N = 20\,000$, i.e., σ_e increased as N increased to 20 000. Therefore, for $\phi_2 \geqslant 0.25$, we first computed σ_e for the systems with $N = 500$, 1000, 2000, 5000, 10 000, and 20 000 and then extrapolated to the $N \to \infty$ limit.

Compared to previous simulation techniques, the Brownian motion simulation algorithm yields accurate values of σ_e with a relatively fast execution time (e.g., on average, the calculations required 4–10 CPU hours on the CRAY Y-MP), especially considering the large system sizes used here. Our calculations were carried out on a VAX station 3100 and on a CRAY Y-MP.

TABLE I. Brownian motion simulation data for the scaled conductivity σ_e/σ_1 of random distributions of overlapping spheres of conductivity σ_2 in a matrix of conductivity σ_1 for $\alpha = \sigma_2/\sigma_1 = 10$ for selected values of the sphere volume fraction in the range $0 < \phi_2 \leqslant 0.8$. Included in the table are the rigorous three-point bounds for overlapping spheres (Refs. 6, 7, and 17) and the exact simulation data for σ_e/σ_1 of equilibrium distribution of hard spheres (Ref. 11).

ϕ_2	Simulation data	Three-point lower bound[a] $\sigma_L^{(3)}/\sigma_1$	Three-point upper bound[a] $\sigma_U^{(3)}/\sigma_1$	Δ	γ_L/Δ	Hard-sphere results[b]
0.2	1.64	1.57	1.74	0.17	0.41	1.54
0.25	1.86	1.76	2.02	0.26	0.38	···
0.4	2.73	2.47	3.05	0.58	0.45	2.41
0.6	4.63	3.94	4.90	0.96	0.72	3.87
0.8	7.11	6.33	7.24	0.91	0.86	···

[a]References 6, 7, and 17.
[b]Reference 11.

IV. RESULTS AND DISCUSSION

In order to test the accuracy of our "template method" for finite α and "pixel method" for $\alpha = \infty$, respectively, we carried out the simulations for a simple cubic array of spheres: an idealized geometry for which exact numerical data are available.[23] The results obtained over a wide range of densities (including near close packing) were found to be exact to three significant figures, confirming that the Brownian motion algorithm can be used in conjunction with the template and pixel methods to compute accurately the effective conductivity of distributions of overlapping spheres.

Our simulation data for overlapping spheres will be compared to the best available rigorous bounds (due to Beran[6] and Milton[7]) on the effective conductivity for this model computed by Torquato and Stell.[17] These authors[17] evaluated three-point upper[6] and lower[7] bounds on σ_e, i.e.,

$$\sigma_L^{(3)} \leqslant \sigma_e \leqslant \sigma_U^{(3)}, \tag{13}$$

where

$$\sigma_U^{(3)} = \sigma_1\phi_1 + \sigma_2\phi_2 - \frac{\phi_1\phi_2(\sigma_2 - \sigma_1)^2}{3\sigma_1 + (\phi_1 + 2\zeta_2)(\sigma_2 - \sigma_1)}, \tag{14}$$

and

$$\sigma_L^{(3)} = \sigma_1\left(\frac{1 + (1 + 2\phi_2)\beta_{21} - 2(\phi_1\zeta_2 - \phi_2)\beta_{21}^2}{1 + \phi_1\beta_{21} - (2\phi_1\zeta_2 + \phi_2)\beta_{21}^2}\right). \tag{15}$$

Here $\phi_1 = 1 - \phi_2$, $\beta_{21} = (\alpha - 1)/(\alpha + 2)$, and ζ_2 is a microstructural parameter that is a multidimensional integral over a three-point statistical correlation function. For subsequent discussion, it is convenient to introduce the following quantities, which involve the bounds:

$$\Delta = (\sigma_U^{(3)}/\sigma_1) - (\sigma_L^{(3)}/\sigma_1), \tag{16}$$

$$\gamma_L = (\sigma_e/\sigma_1) - (\sigma_L^{(3)}/\sigma_1), \tag{17}$$

$$\gamma_U = (\sigma_U^{(3)}/\sigma_1) - (\sigma_e/\sigma_1). \tag{18}$$

The quantity Δ is the bound width made dimensionless with the conductivity of the matrix σ_1. The quantities γ_L and γ_U are the absolute differences between the exact dimensionless effective conductivity and lower and upper bounds, respectively.

For arbitrary composite media, it has been observed by Torquato[24] that when one phase is much more conducting than the other, say $\sigma_2 \gg \sigma_1$, lower bounds are expected to yield good estimates of σ_e/σ_1 provided that $\phi_2 < \phi_2^c$ (where ϕ_2^c is the percolation threshold of phase 2) and that the average cluster size of phase 2 Λ_2 is much smaller than the system size L. Thus, even though the bound width Δ is very large when $\sigma_2 \gg \sigma_1$ (and, indeed, goes to infinity in the limit $\sigma_2/\sigma_1 \to \infty$), lower bounds should give a reasonable estimate of σ_e (i.e., $\gamma_L \ll 1$) provided that $\Lambda_2 \ll L$. Similarly, upper bounds are expected to yield useful estimates of σ_e for $\sigma_2 \gg \sigma_1$ when $\phi_2 > \phi_2^c$ and $\Lambda_1 \ll L$, where Λ_1 is the average of cluster size of phase 1. For the special case of overlapping spheres, the average cluster is composed of approximately 10 particles[15] at $\phi_2 = 0.2$. As ϕ_2 increases beyond $\phi_2 = 0.2$, the size of the average cluster grows precipitously until it becomes infinitely large at the threshold value of $\phi_2^c \simeq 0.3$. At $\phi_2 = 0.28$, for example, the average cluster consists of approximately 150 particles.[15] Thus, for the model under consideration, it may be argued that the condition $\Lambda_2 \ll L$ holds when $0 \leqslant \phi_2 \leqslant 0.2$. On the other hand, phase 1 (matrix) ceases to percolate[16] at $\phi_2 \simeq 0.97$. Thus, the condition $\Lambda_1 \ll L$ holds in the vicinity of $\phi_2 = 1$.

We chose to examine three different contrast values for the cases of conducting spheres ($\alpha > 1$), i.e., $\alpha = 10$, 50, and ∞. Our simulation data for $\alpha = 10$ together with the rigorous three-point bounds are presented in Table I and Fig. 5. Included in Fig. 5 is Torquato's approximation (19) and included in Table I are the bound quantities Δ and γ_L and the simulation results for the effective conductivity of the distributions of hard spheres due to Kim and Torquato.[11] It is seen that the overlapping-sphere data always lie between the upper and lower bounds. Although α is not much greater than unity here, the data lie closer to the lower bound for $\phi_2 \leqslant \phi_2^c \simeq 0.3$ and lie closer to the upper bound for $\phi_2 > 0.3$. Not surprisingly, the effective conduc-

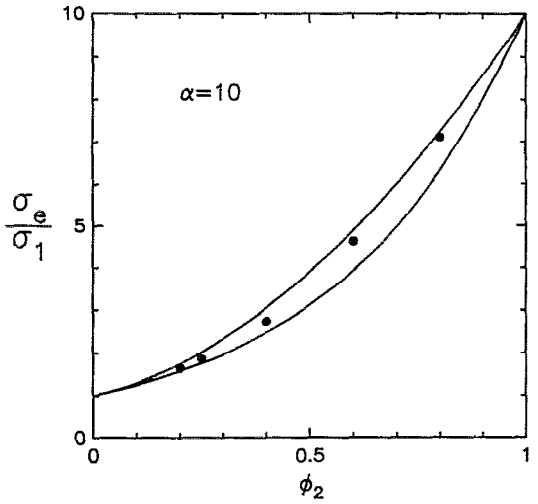

FIG. 5. Scaled effective conductivity σ_e/σ_1 of an equilibrium distribution of overlapping spheres in a matrix for $\alpha = 10$. Solid lines are rigorous three-point bounds (see Refs. 6 and 7) and filled circles are our simulation data.

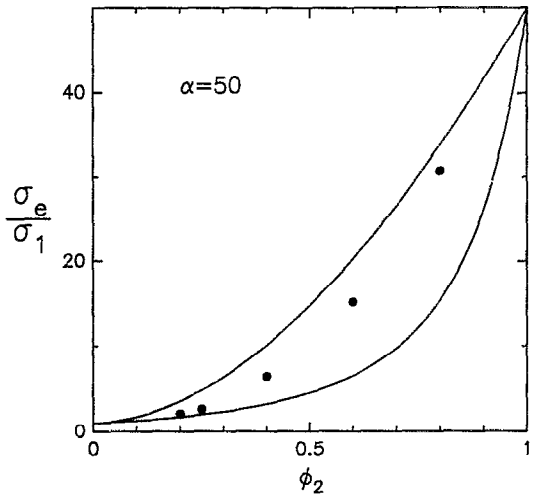

FIG. 6. Scaled effective conductivity σ_e/σ_1 of an equilibrium distribution of overlapping spheres in a matrix for $\alpha = 50$. Solid lines are rigorous three-point bounds (see Refs. 6 and 7) and filled circles are our simulation data.

tivity for overlapping spheres is always higher than for hard spheres at the same volume fraction. This is because the average cluster size Λ_2 for overlapping spheres is always greater than or equal to Λ_2 for nonoverlapping sheres.

The simulation data and the bounds for the case $\alpha = 50$ are summarized in Table II and Fig. 6. Figure 6 includes Torquato's approximation (19) and Table II includes the quantities Δ and γ_L. It is seen that the data always lie within the bounds. For $\phi_2 < \phi_2^c$, the data lie closer to the lower bound, and indeed for $\phi_2 \leqslant 0.2$ the lower bound provides a good estimate of σ_e/σ_1, consistent with observations of Torquato.[24] On the other hand, for $\phi_2 > 0.42$, the data lie closer to the upper bound. It is interesting to note that a simple linear interpolation formula based upon the upper and lower bounds for $\alpha > 1$ and $\phi_2 > \phi_2^c$ can be obtained which accurately estimates the conductivity data[25] for this range of parameters.

The case of superconducting overlapping spheres ($\alpha = \infty$) is presented in Table III and Fig. 7. Figure 7 includes an approximation due to Torquato[24] which also depends on the microstructural parameter ζ_2, namely,

$$\frac{\sigma_e}{\sigma_1} = \frac{1 + 2\phi_2\beta_{21} - 2\phi_1\zeta_2\beta_{21}^2}{1 - \phi_2\beta_{21} - 2\phi_1\zeta_2\beta_{21}^2}. \tag{19}$$

Relation (19) should provide an excellent estimate of σ_e provided that the dispersed phase 2 does not possess large connected substructure. This condition will be met for $\phi_2 \leqslant 0.2$ as discussed above. Table III includes the quantity γ_L and our simulation data for hard spheres.[11] The upper bound is not shown since it is infinite in this instance. Nonetheless, the approximation (19) and lower bound provide a good estimate of σ_e/σ_1 for $\phi_2 \leqslant 0.2$, which again is consistent with Torquato's observations.

Table IV and Fig. 8 show our simulation results for the case of the distributions of the insulating ($\alpha = 0$) spheres. Here we compare our results to the rigorous upper bound (14) and the exact results for the corresponding case of hard spheres.[11] The lower bound vanishes for $\alpha = 0$. It is

TABLE II. Brownian motion simulation data for the scaled conductivity σ_e/σ_1 of random distributions of overlapping sheres of conductivity σ_2 in a matrix of conductivity σ_1 for $\alpha = \sigma_2/\sigma_1 = 50$ for selected values of the sphere volume fraction in the range $0 < \phi_2 \leqslant 0.8$. Included in the table are the rigorous three-point bounds.[a]

ϕ_2	Simulation data	Three-point lower bound[a] $\sigma_L^{(3)}/\sigma_1$	Three-point upper bound[a] $\sigma_U^{(3)}/\sigma_1$	Δ	γ/Δ
0.2	2.16	1.78	3.60	1.62	0.23
0.25	2.67	2.06	4.87	2.81	0.22
0.4	6.44	3.28	10.11	6.83	0.46
0.6	15.16	6.54	20.29	13.75	0.63
0.8	30.74	15.33	33.81	18.48	0.83

[a]References 6, 7, and 17.

TABLE III. Brownian motion simulation data for the scaled conductivity σ_e/σ_1 of random distributions of superconducting overlapping spheres in a matrix ($\alpha = \infty$) for selected values of the sphere volume fraction in the range $0 < \phi_2 \leqslant 0.28$. Included in the table are the rigorous three-point lower bound for overlapping spheres[a] and the exact simulation data for σ_e/σ_1 of equilibrium distribution of hard spheres.[b]

ϕ_2	Simulation data	Three-point lower bound[a] $\sigma_L^{(3)}/\sigma_1$	Hard-sphere results[b]
0.1	1.38	1.35	...
0.15	1.70	1.58	...
0.2	2.25	1.85	1.83
0.25	3.36	2.17	...
0.27	4.27	2.41	...
0.28	5.31	2.49	...

[a]References 7 and 17.
[b]Reference 11.

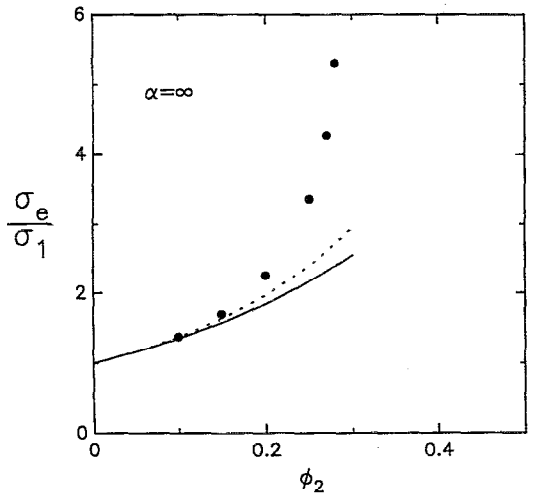

FIG. 7. Scaled effective conductivity σ_e/σ_1 of an equilibrium distribution of superconducting overlapping spheres ($\alpha = \infty$) in a matrix. The solid line is the rigorous three-point lower bound (see Ref. 7) the dotted line is an approximation due to Torquato (see Ref. 24). The filled circles are our simulation data.

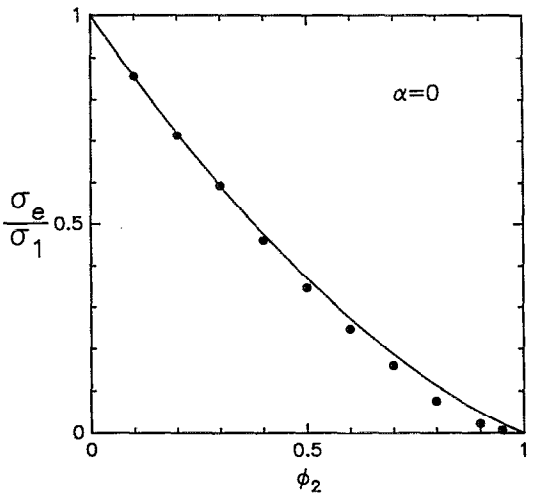

FIG. 8. Scaled effective conductivity σ_e/σ_1 of an equilibrium distribution of insulating overlapping spheres ($\alpha = 0$) in a matrix. The solid line is the rigorous three-point upper bound (see Ref. 6) and the filled circles are our simulation data.

clear that the increased particle-phase connectivity due to overlapping lowers σ_e/σ_1 relative to the hard-sphere case.

It should be noted that Tobochnik, Laing, and Wilson[26] also used a Brownian motion technique to compute σ_e for overlapping spheres, but only reported results for the extreme contrast values of $\alpha = 0$ and $\alpha = \infty$. Their methodology differs from our technique in two basic ways, however. First, when the Brownian tracer is near to a smooth interface as in Fig. 2(a), we use the accurate analytical expression (7) for the mean hitting time τ_s while they simply approximated, in the language of this paper, $\tau_s = (1 + A_2/A_1)R^2/6\sigma_1$ for $\alpha = 0$. This is, in fact, a further approximation to the expression (10) for τ_s which, in turn, is already a modification of Eq. (7) and which we use only when the first-passage sphere encompasses complex intersecting surfaces [as illustrated in Fig. 2(b)]. Second, they used the aforementioned approximation whenever a Brownian tracer encounters the interface regardless of its shape. Since their approximation of the area ratio A_2/A_1 instead of the volume ratio V_2/V_1 is independent of, and hence is not properly reflecting, the detailed inner structure of the first-passage sphere, then the resulting data obtained by their alogorithm are expected to involve more errors as the interface boundary becomes more complex, which is the case for the distributions of the overlapping spheres. Note that p_1 and p_2 need not be calculated when $\alpha = 0$. Comparison of our simulation data to theirs, which are not shown here, revealed that their data are slightly lower than ours.

TABLE IV. Brownian motion simulation data for the scaled conductivity σ_e/σ_1 of random distributions of insulating overlapping spheres ($\alpha = 0$) in a matrix of conductivity σ_1 for selected values of the sphere volume fraction in the range $0 < \phi_2 \leq 0.95$. Included in the table are the rigorous three-point upper bound for overlapping spheres[a] and the exact simulation data for σ_e/σ_1 of equilibrium distribution of hard spheres.[b]

ϕ_2	Simulation data	Three-point upper bound[a] $\sigma_U^{(3)}/\sigma_1$	Δ	γ_U/Δ	Hard-sphere results[b]
0.1	0.855	0.855	0.855	0.000	···
0.2	0.714	0.719	0.719	0.007	0.724
0.3	0.593	0.593	0.593	0.000	···
0.4	0.461	0.476	0.476	0.032	0.491
0.5	0.346	0.370	0.370	0.065	···
0.6	0.248	0.274	0.274	0.095	0.287
0.7	0.160	0.188	0.188	0.149	···
0.8	0.0760	0.113	0.113	0.327	···
0.9	0.0222	0.0496	0.0496	0.552	···
0.95	0.0063	0.0227	0.0227	0.722	···

[a]References 6 and 17.
[b]Reference 11.

In the case $\alpha = \infty$, Tobochnik and co-workers[26] used another approximation for the mean hitting time τ_s. They approximated the mean hitting time, in the language of this paper, by the relation $\tau_s = \delta_2^2 a^2/2\sigma_1$ in contrast to Eq. (11). Their approximation underestimates τ_s and hence leads to an overestimation of σ_e/σ_1. This is easily proved in the case of a spherical monomer since the exact expression[10] is given by, for negligibly small δ_1,

$$\tau_s = \frac{a^2}{6\sigma_1}[(1+\delta_2)^2 - 1] = \frac{\delta_2^2 a^2}{2\sigma_1} + \frac{a^2}{6\sigma_1}\delta_2(1-\delta_2). \tag{20}$$

It is evident from Eq. (20) that the approximation of Tobochnik and co-workers underestimates τ_s and therefore overestimates σ_e, since δ_2 is always taken to be less than unity. (In this study, it is taken to be 0.01.) To further support our claim that the algorithm of Tobochnik and co-workers overestimates σ_e for $\alpha = \infty$, we computed σ_e for a simple cubic array using their algorithm with $\delta_1 = 0.0001$ and $\delta_2 = 0.01$. As noted earlier, this is a useful benchmark model since exact results are available.[23] Their algorithm yields $\sigma_e/\sigma_1 = 3.28$ at $\phi_2 = 0.3$ and $\sigma_e/\sigma_1 = 11.77$ at $\phi_2 = 0.5$. This is to be compared to exact re-

sults of $\sigma_e/\sigma_1 = 2.33$ at $\phi_2 = 0.3$ and $\sigma_e/\sigma_1 = 5.89$ at $\phi_2 = 0.5$. Our algorithm in contrast predicts the exact results to three significant figures. In the case of overlapping spheres, for example, Tobochnik and co-workers found that $\sigma_e/\sigma_1 \simeq 8.5$ (within the scale of their figure) at $\phi_2 = 0.25$, whereas we obtained that $\sigma_e/\sigma_1 = 3.36$ at $\phi_2 = 0.25$. Note that as explained earlier, p_1 and p_2 need not be calculated for $\alpha = \infty$.

V. CONCLUDING REMARKS

The general first-passage-time technique developed by the authors earlier[10–12] has been applied to compute the effective conductivity σ_e of the distributions of overlapping spheres. To facilitate the calculation for generally irregularly shaped interfaces, the "template method" for nonsuperconducting clusters and the "pixel method" for superconducting clusters were developed and applied. The simulation procedure was shown to yield highly accurate estimates of conductivity for benchmark models. Our calculations of σ_e for overlapping spheres always lie between three-point bounds and, to our knowledge, are the most accurate and comprehensive data for this model obtained to date. Consistent with the observations of Torquato,[24] one of the bounds yields a good estimate of σ_e, even in the extreme cases of $\alpha = 0$ and $\alpha = \infty$, depending upon the size of the average cluster. Because the average cluster size in overlapping spheres is larger than for equilibrium hard spheres[11] at the same volume fraction, the effective conductivity of the former system is larger (smaller) than σ_e for the latter system when $\alpha > 1$ ($\alpha < 1$).

ACKNOWLEDGMENTS

The authors gratefully acknowledge the support of the Office of Basic Energy Sciences, U.S. Department of Energy, under Grant No. DE-FG05-86ER13482. Some computer resources (CRAY Y-MP) were supplied by the North Carolina Supercomputing Center funded by the State of North Carolina.

[1] Z. Hashin, J. Appl. Mech. **50**, 481 (1983).
[2] S. Torquato, Appl. Mech. Rev. **44**, 37 (1991).
[3] D. A. Bruggeman, Ann. Phys. **28**, 160 (1937).
[4] A. Acrivos and E. Chang, Phys. Fluids **29**, 1 (1986).
[5] Z. Hashin and S. Shtrikman, J. Appl. Phys. **33**, 3125 (1962).
[6] M. Beran, Nuovo Cimento **38**, 771 (1965).
[7] G. W. Milton, J. Appl. Phys. **52**, 5294 (1981).
[8] C. A. Miller and S. Torquato, J. Appl. Phys. **68**, 5486 (1990).
[9] P. P. Durand and L. H. Ungar, Int. J. Num. Methods Eng. **26**, 2487 (1988).
[10] I. C. Kim and S. Torquato, J. Appl. Phys. **68**, 3892 (1990).
[11] I. C. Kim and S. Torquato, J. Appl. Phys. **69**, 2280 (1991).
[12] I. C. Kim and S. Torquato, Phys. Rev. A **43**, 3198 (1990).
[13] R. T. Bonnecaze and J. F. Brady, Proc. R. Soc. London Ser. A **430**, 285 (1990).
[14] J. G. Berryman, Phys. Rev. A **27**, 1053 (1983).
[15] S. W. Haan and R. Zwanzig, J. Phys. A **10**, 1547 (1977); E. M. Sevick, P. A. Monson, and J. M. Ottino, J. Chem. Phys. **88**, 1198 (1988); S. B. Lee and S. Torquato, J. Chem. Phys. **89**, 6427 (1988).
[16] J. Kertesz, J. Phys. Lett. (Paris) **42**, L393 (1981); W. T. Elam, A. R. Kerstein, and J. J. Rehr, Phys. Rev. **52**, 1516 (1984).
[17] S. Torquato and G. Stell, Lett. Appl. Eng. Sci. **23**, 375 (1985); J. Chem. Phys. **79**, 1505 (1983). These references actually report tabulations of the parameter I_1 which is related to ζ_2 by the simple relation $\zeta_2 = 1 - 9I_1/2\phi_1\phi_2$.
[18] H. L. Weissberg, J. Appl. Phys. **34**, 2636 (1963); H. L. Weissberg and S. Prager, Phys. Fluids **13**, 2958 (1970); S. Torquato, G. Stell, and J. D. Beasley, Lett. Appl. Eng. Sci. **23**, 365 (1985); J. G. Berryman, J. Phys. D **18**, 585 (1985); S. Torquato, J. Chem. Phys. **84**, 6345 (1986).
[19] See, for example, Y. C. Chiew and E. D. Glandt, J. Phys. A **16**, 2599 (1983); S. B. Lee, and S. Torquato, J. Chem Phys. **91**, 1173 (1989), and references therein.
[20] P. A. Smith and S. Torquato, J. Comput. Phys. **76**, 176 (1988).
[21] J. Hoshen and R. Kopelman, Phys. Rev. B **28**, 5323 (1983).
[22] S. B. Lee and S. Torquato, J. Chem. Phys. **89**, 3258 (1988).
[23] D. R. McKenzie, R. C. McPhedran, and G. H. Derrick, Proc. R. Soc. London Ser. A **362**, 211 (1978).
[24] S. Torquato, J. Appl. Phys. **58**, 3790 (1985).
[25] For $\alpha > 1$ and $\phi_2 > \phi_2^c$, a simple interpolation formula based upon the upper and lower bounds can be employed to accurately estimate the effective conductivity σ_e. Specifically, the expression $\sigma_e/\sigma_1 = \sigma_L^{(3)}/\sigma_1 + \Delta(1 - 2\phi_2^c + \phi_2)/[2(1 - \phi_2^c)]$ yields estimates of σ_e that are very close to the simulation data for $\alpha > 1$ and $\phi_2 > \phi_2^c$. Recall that Δ is given by Eq. (14).
[26] J. Tobochnik, D. Laing, and G. Wilson, Phys. Rev. A **41**, 3052 (1990).